


 Cite this: *RSC Adv.*, 2026, 16, 19412

Screening and identification of a new antimicrobial, *Streptomyces rehmanniae*, from the rhizosphere of *Rehmannia glutinosa*

 Hairong He,^a Tong Wang,^a Jiaqi Li,^a Chen Sun,^a Zhaoxu Ma,^b Zhenzhu Zhao,^a Xiaoke Zheng^{*a} and Pengqiang Du^{*c}

Objectives: we aimed to isolate and characterize antimicrobial-producing strains from the rhizosphere soil of *Rehmannia glutinosa*, with the goal of identifying novel antimicrobial agents to address the escalating crisis of antimicrobial resistance. **Methods:** strain Rer75 was isolated from rhizosphere soil and characterized based on morphology, phylogenetic analyses, average nucleotide identity (ANI), and digital DNA–DNA hybridization (dDDH). Bioactive compounds were extracted and purified from the strain. The antimicrobial activity of isolated compounds was evaluated against *E. coli* CGMCC 1.1521, *S. aureus* ATCC 25923, and the pathogenic fungus *B. berengeriana* CFCC 85789. Genome mining was performed using antiSMASH to identify biosynthetic gene clusters (BGCs). Inhibition of key genes in the nigericin-like gene cluster was performed to elucidate the relationship between the antibacterial activity of the strain and the gene cluster. **Results:** strain Rer75, identified as a novel species named “*Streptomyces rehmanniae*”, exhibited strong antagonistic activity against six types of plant pathogenic fungi. Seven compounds were isolated from its crude extract, including a new unsaturated hydroxy ester (compound 1) and six known compounds (compounds 2–7). Compound 1 showed moderate antibacterial activity against *E. coli* and *S. aureus*, but no activity against *B. berengeriana*. Genomic analyses revealed 40 BGCs encoding polyketides, nonribosomal peptides, and terpenes, many of which displayed low similarity to known clusters. Notably, the nigericin-like BGC No. 37 was essential for the antibacterial activity of the strain. **Conclusions:** *Streptomyces rehmanniae* Rer75 is a promising source of novel antimicrobial compounds. The genomic insights into its diverse and unique biosynthetic potential highlight its ecological and biotechnological importance for developing new antimicrobial agents.

 Received 17th October 2025
 Accepted 23rd March 2026

DOI: 10.1039/d5ra07947k

rsc.li/rsc-advances

1 Introduction

Antimicrobial resistance (AMR) has emerged as one of the greatest global concerns in the 21st century. It occurs when pathogens, including bacteria, fungi, parasites, and viruses, adapt and become resistant to drugs (e.g., antibiotics).^{1,2} It has been reported that AMR-related deaths surpassed 1.2 million in 2019, and projections warn of a staggering increase to 10 million by 2050 if containment efforts remain inadequate.¹

One major contributing factor is the irresponsible use of antibiotics across multiple sectors, including human medicine, agriculture, animal health, and the food industry.² Other important reasons include the rapid growth of AMR infection rates and the lack of new antimicrobial medications being

introduced to combat this issue.¹ Thus, the discovery and development of novel antimicrobial compounds is an immediate priority.

Plant diseases caused by fungal and bacterial phytopathogens is a significant challenge in agriculture. Chemical control is the main approach for managing plant diseases.³ In crops in which chemical pesticides are not used, global losses due to plant diseases are estimated to be nearly 20%.^{4,5} However, the irrational use of chemical pesticides has led to increased microbial resistance.⁶ At the same time, pesticide residues in the environment pose threats to human and environmental health, compelling us to seek eco-friendly biopesticides and novel antimicrobial agents for the biocontrol of plant diseases.

Streptomyces species are the primary source of bioactive specialized metabolites used in research and medicine. They include many antimicrobials, mostly beneficial microorganisms that are abundant in plant rhizosphere soil.⁷ In recent years, rhizosphere *Streptomyces* species have attracted considerable attention for biological control of pathogen growth through the release of antibiotics, antimicrobial peptides, and the induction of systemic resistance of plants.^{8,9} Thus,

^aCollege of Pharmacy, Henan University of Chinese Medicine, Zhengzhou 450046, China. E-mail: zhengxk.2006@163.com

^bCollege of Life Science, China West Normal University, Nanchong City, Sichuan 637009, China

^cCollege of Plant Protection, Henan Agricultural University, Zhengzhou 450046, China. E-mail: dupengq@163.com


Streptomyces species are important sources for the isolation of new compounds as clinical drugs. However, over the past half century, the screening of common *Streptomyces* strains has led to repeated isolation of known active compounds, making it challenging to discover new active compounds.¹⁰ Therefore, an important approach to address these concerns is to mine new *Streptomyces* strains and search for novel genes and products.¹¹

During an ongoing study investigating bioactive compound-producing actinomycetes, a *Streptomyces*-like strain, designated “strain Rer75”, was isolated from the rhizosphere of *Rehmannia glutinosa*, a widely used traditional Chinese herb with very high medicinal value.¹² Morphological characteristics, phenotypic properties, chemotaxonomic characteristics, and genomic data were used to characterize the taxonomic position of strain Rer75 that was identified as a new species of *Streptomyces*. Besides, the medium for fermentation of novel compounds was selected, and compounds isolated from Rer75 were tested for their antimicrobial activities. In our study, the new strain Rer75 is a potential material for the isolation of novel antimicrobial compounds. Its genome sequence data will be useful to elucidate the biosynthetic and regulatory mechanisms for the secondary metabolites that could be used in biotechnology and natural product biosynthesis.

2 Materials and methods

2.1 Antifungal activity assay of strain Rer75

Strain Rer75 was isolated from the rhizosphere soil of *R. glutinosa*¹² and deposited in the China Center for Type Culture Collection (CCTCC NO. M 20231749) (Fig. S1). Strain Rer75 was cultured on ISP 3 medium at 28 °C for 6 d prior to antifungal assays. Its antagonistic activity against six fungal pathogens (*Botryosphaeria berengeriana* CFCC 85789, *Verticillium dahliae* Kleb. ACCC 36203, *Fusarium graminearum* Schw. ACCC 37408, *Colletotrichum orbiculare* ACCC 36060, *Exserohilum turcicum* CGMCC 3.7336, *Fusarium oxysporum* CGMCC 3.18025) was tested *via* the dual-culture method on V8 medium. Fungal pathogens were pre-cultured on V8 medium at 28 °C for 7 d. For the assay, Rer75 was spot-inoculated on one side of a V8 plate and incubated at 28 °C for 3 d, after which a 7-mm mycelial plug of each pathogen was placed perpendicular to the Rer75 colony. Following 5–7 d of co-incubation, antifungal activity was calculated as described previously.¹³

2.2 Taxonomic characterization of strain Rer75

Chromosomal DNA was extracted and PCR-amplified following standard protocols. The purified PCR product was cloned into the pMD19-T vector (Takara Biotechnology) and sequenced on the Applied Biosystems 3730XL DNA sequencer. The near full-length 16 S rRNA gene sequence (1527 bp) was subjected to similarity analyses using the EzBioCloud database (<https://www.ezbiocloud.net>). Sequence alignment was conducted with CLUSTAL X 1.83 against GenBank/EMBL/DBJ reference sequences with complete deletion of gaps and missing data. A neighbor-joining phylogenetic tree was constructed in MEGA X under the Kimura two-parameter model,¹⁴ with topological

stability evaluated by 1000 bootstrap replicates. A whole-genome phylogenetic tree was built using the Type Strain Genome Server (TYGS). Digital DNA–DNA hybridization (dddH) values were calculated for taxonomic assignment.¹⁵ Average nucleotide identity (ANI) values between strain Rer75 and its closely related species were determined *via* JSpeciesWS.¹⁶

2.3 Morphological, physiological, and chemotaxonomic characterizations

Morphological characteristics were observed on diverse media (ISP series, Bennett's, and nutrient agar) after 14-d incubation at 28 °C. Spore morphology was examined *via* scanning electron microscopy (Hitachi SU8010). The growth profile of strain Rer75 was evaluated at 4, 10, 20, 25, 28, 37, 40 and 45 °C on ISP 3 agar over 14 d. Tolerance to pH (2–12, 1-unit intervals) and NaCl (0–10%, 1-unit intervals) was assessed in GY broth with rotary shaking at 28 °C for 14 d. Physiological traits, including utilization of sole carbon/nitrogen sources (0.5% w/v), milk peptonization and coagulation, cellulose decomposition, nitrate reduction, gelatin liquefaction, H₂S and protease production, tween hydrolysis and urease activity were determined following established protocols.¹⁷ Chemotaxonomic analyses (cell-wall amino acids, whole-cell glycogen, polar lipids, menaquinones) were performed as described.^{18,19}

2.4 Whole genome sequencing and analyses for the secondary metabolites of Rer75

Strain Rer75 was cultured in ISP 2 liquid medium for 3 d at 28 °C to obtain mycelia. Genomic DNA was extracted using the Invitrogen PureLink[®] Genomic DNA Kit, and its quality and quantity were assessed using the NanoDrop ND-1000 Spectrophotometer (Thermo Fisher Scientific). Upon confirmation of high-quality DNA, whole-genome sequencing was performed on the nanopore sequencing platform. The genome was assembled *de novo* with Canu and polished with Pilon.^{20,21} Annotation was done using NCBI PGAP and RAST 2.0.^{22,23} Biosynthetic gene clusters (BGCs) were predicted with antiSMASH v6.0.²⁴

2.5 Repressed expression core gene in gene cluster no. 37

To verify the function of gene cluster no. 37 (a nigericin-like cluster with 90% identity), a CRISPR-Cpf1-mediated gene inhibitory plasmid pSETddCpf1 was employed.²⁵ Based on the PAM sequence (TTV) recognized by Cpf1, appropriate sgRNA sequences were screened in the open reading frame of *ctg_8048*

Table 1 Primers used in this study

| Primer | Sequences |
|----------|---|
| cr-RNA-F | GGAATTCATATGTGGATCCT ACCAACCGGCACGATT |
| R8048-R | GACTAGTCGTGCGCGGAGGAGCGCG TCAAATCTACAACAGTAGAAATTTGG |
| Apr-SE | CATGCCCTCGTGGTCAGGT |
| Apr-AN | TCTTCGCATCCGCCTCT |



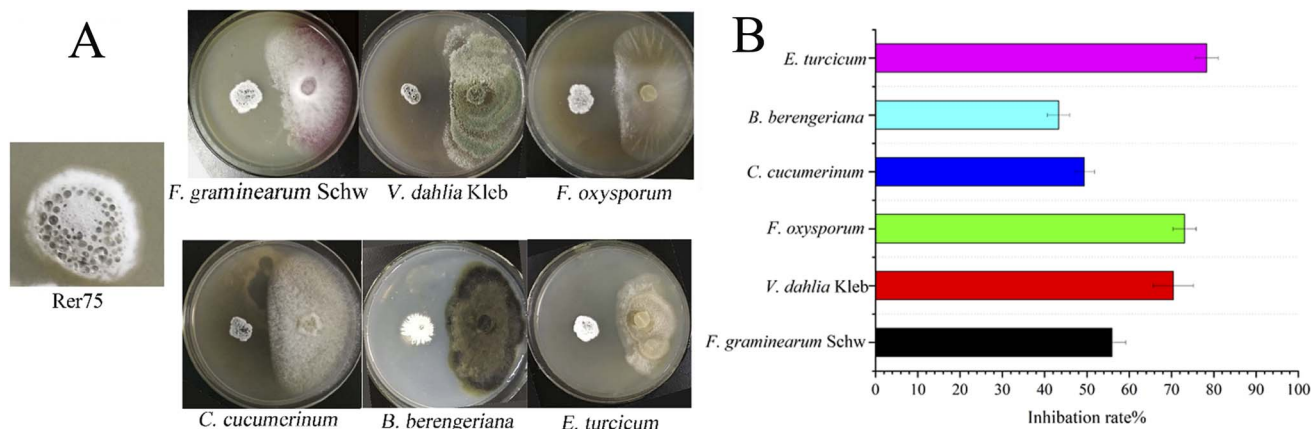


Fig. 1 Broad-spectrum antimicrobial activities of Rer75. (A) Inhibitory effect of Rer75 against six types of fungi. (B) Statistical analyses of the percent inhibition of Rer75 for each pathogen.

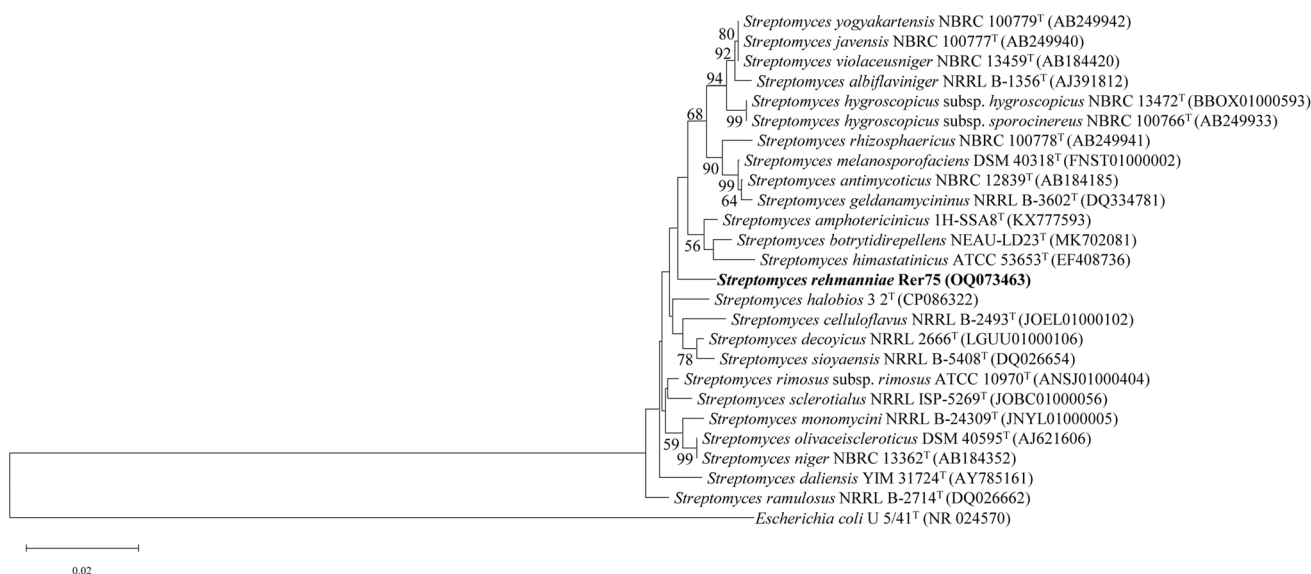


Fig. 2 Neighbor-joining tree based on 16 S rRNA gene sequences showing the relationship between strain Rer75 (1527 bp) and related species of the genus *Streptomyces*. Bootstrap percentages ($\geq 50\%$) based on 1000 replications are listed at nodes. Bar, 0.0020 substitutions per nucleotide position.

(the core gene of cluster no. 37). Using pSETddCpf1 as a template, crRNA expression cassette fragments were amplified with primer cr-RNA-F and specific primer R8048R containing 23-base sgRNA fragments (Table 1). The amplified fragment was double-digested with *Nde*I and *Spe*I, then ligated into the corresponding sites of pSETddCpf1 using T4 DNA ligase to construct the gene suppression plasmid pSETddCpf1-R8048. This plasmid was introduced into strain Rer75 *via* conjugation to generate candidate exconjugants. Primers Apr-SE and Apr-AN were employed to amplify the antibiotic resistance gene (*Apm^R*) that stabilizes genomic integration of the plasmid (Table 1), yielding positive exconjugants. Positive exconjugant Rer75-R8048 and the wild-type strain Rer75 were fermented separately. Bioactivity assays were conducted to compare broth activity differences, clarifying the role of the target cluster in metabolite synthesis and activity regulation. In addition, the

plate confrontation assay was performed to verify the antifungal activity of the metabolites synthesized by this gene cluster.

2.6 Screening medium for isolation compounds

Rer75 was fermented in eight media (GYM I, GYM III, ISP 2, HZ-2, GY, HZ-1, MB, H9) (Table S1). The antimicrobial activity of extracts (supernatant and pellet) from each medium was tested against bacterial (*E. coli* CGMCC 1.1521 and *S. aureus* ATCC 25923) and fungal (*B. berengeriana* and *F. graminearum* Schw) indicators *via* disc diffusion assays. The medium that yielded the strongest activity was selected for large-scale fermentation.

2.7 Fermentation, extraction, and isolation of compounds

Large-scale fermentation was performed in 50 L of H9 medium. The broth was centrifuged, and the supernatant was extracted



with ethyl acetate. The mycelial pellet was extracted with methanol. The combined crude extract (34 g) was fractionated using medium-pressure liquid chromatography (MPLC) with a methanol–water gradient (v/v 20 : 80, 40 : 60, 60 : 40, 80 : 20, 100 : 0, each 3000 mL), yielding five fractions (a–e). These fractions were further purified using silica gel chromatography (Sephadex LH-20 column) and preparative HPLC to isolate seven compounds (1–7).

Fraction a (3.6 g) was further separated on silica gel and eluted with petroleum ether–acetone (v/v 100 : 10, 100 : 20) to yield six subfractions (a1–a6). Subfraction a1 was subsequently purified using prep-HPLC (C-18) with a gradient eluent [acetonitrile–water (MeCN–H₂O) v/v, 70 : 20 to 100 : 0, over 30 min, flow rate = 3 mL min⁻¹], resulting in the isolation of

compounds 1 (2.1 mg, $t_R = 13$ min), 2 (1.3 mg, $t_R = 18$ min), 3 (1.6 mg, $t_R = 25$ min).

Fraction b (0.6 g) was subjected to a Sephadex LH-20 column (MeOH) to yield three subfractions (b1–b3). Subfraction b2 was subsequently purified using prep-HPLC (C-18) with a gradient eluent [MeCN–H₂O v/v, 25 : 75 to 75 : 25, over 25 min, flow rate = 3 mL min⁻¹], yielding compound 4 (1.8 mg, $t_R = 21$ min).

Fraction c (3.5 g) was fractionated using a Sephadex LH-20 column in methanol to give four subfractions (c1–c4). Compound 5 (1.4 mg, $t_R = 15$ min) and compound 6 (2.1 mg, $t_R = 21$ min) were purified from subfraction c4 using prep-HPLC (C-18) with gradient elution [MeCN–H₂O v/v, 25 : 75 to 65 : 35, over 27 min, flow rate = 3 mL min⁻¹].

Fraction e (2.5 g) was fractionated using a Sephadex LH-20 column in methanol to give three subfractions (e1–e3).

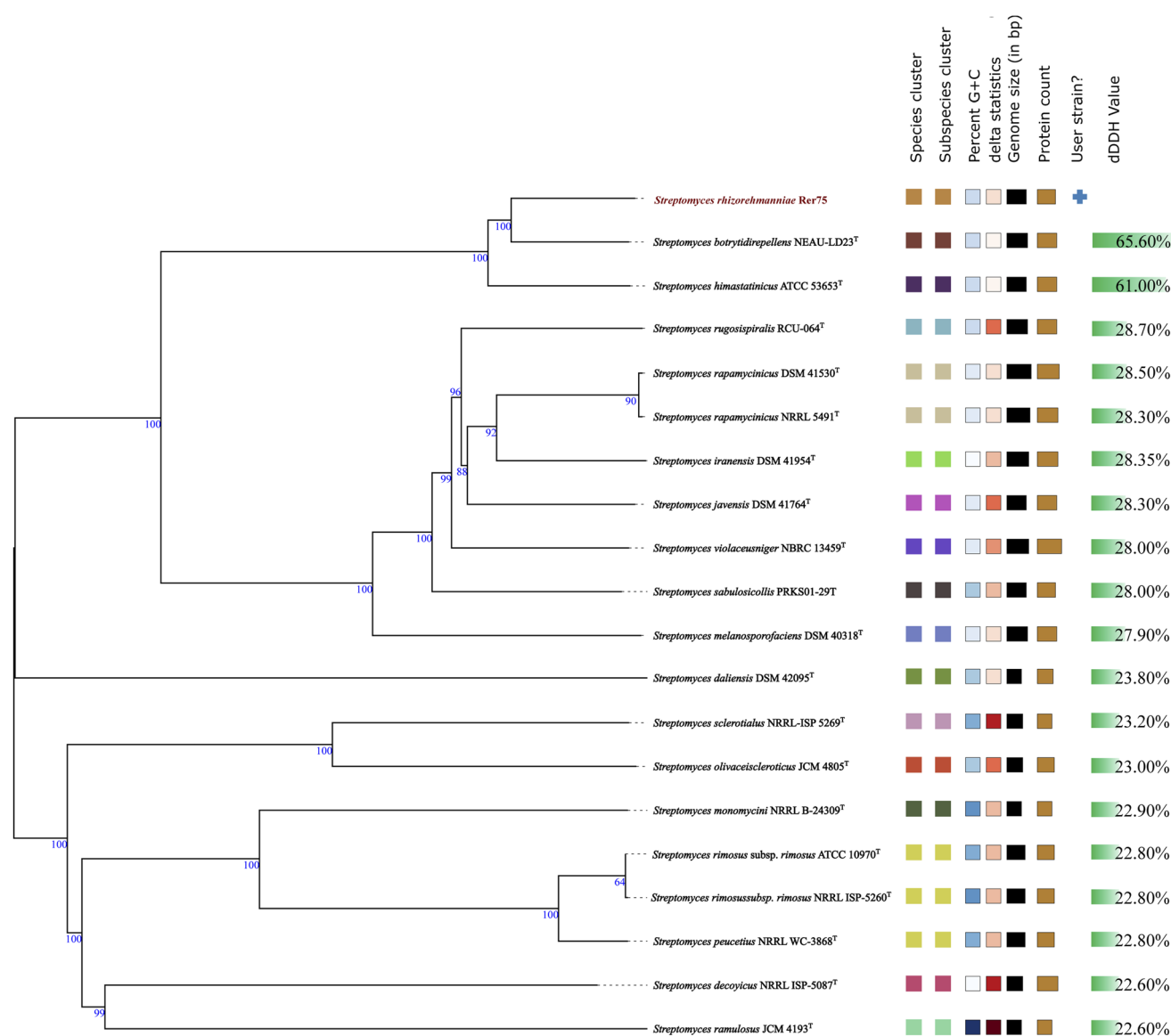


Fig. 3 Whole-genome sequence tree generated with TYGS for strain Rer75 and closely related *Streptomyces* species. Tree inferred with FastME from GBDP distances calculated from genome sequences. Branch lengths are scaled in terms of the GBDP distance formula d5; numbers above branches are GBDP pseudo-bootstrap support values from replications; digital DNA–DNA hybridization (dDDH) values are provided. T: type strain.



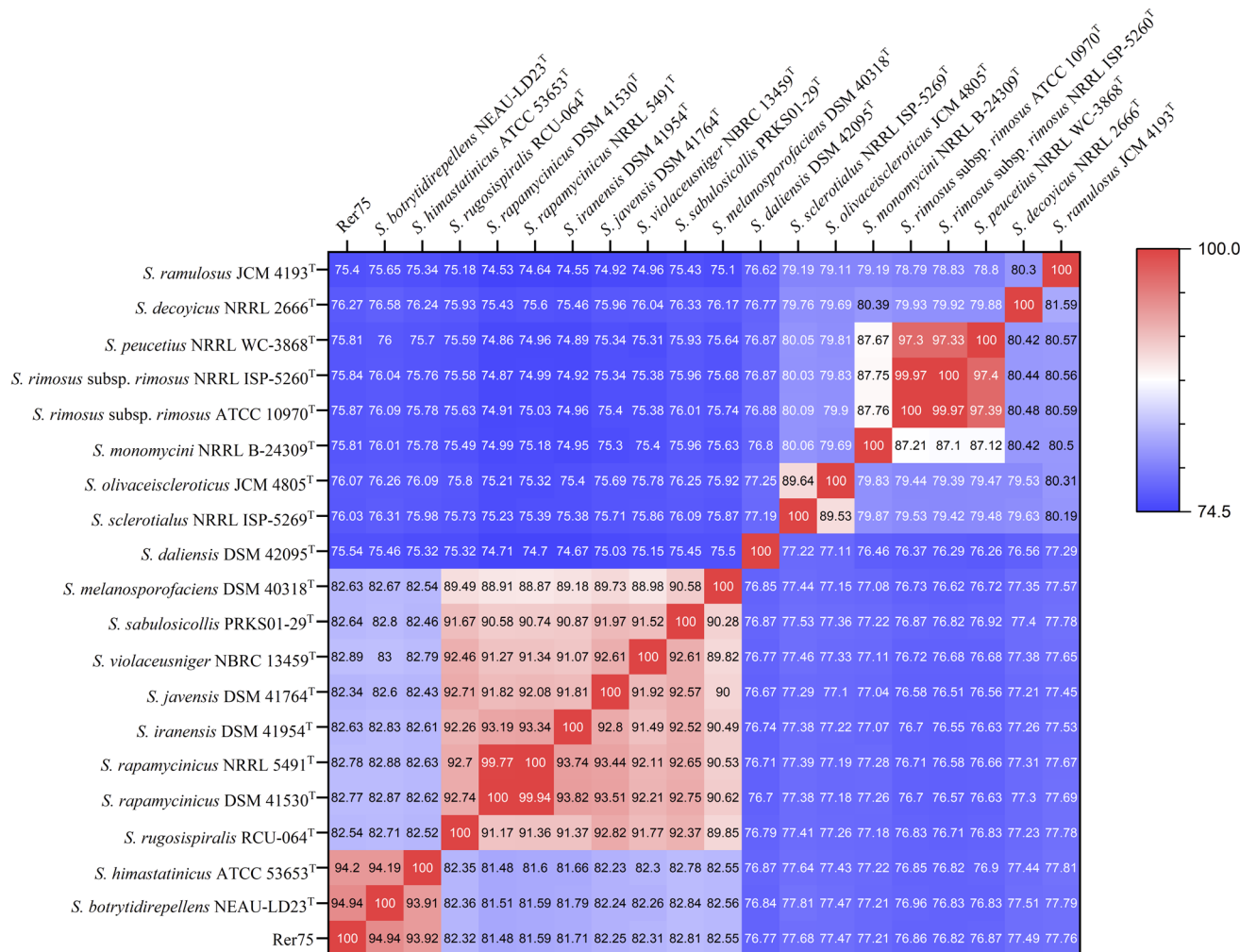


Fig. 4 Average nucleotide identity (ANI) calculated using the BLAST-based orthoANI heatmaps of Rer75 and other closely related *Streptomyces* species.

Compound 7 (1.2 mg, $t_R = 12$ min) was purified from sub-fraction e2 using prep-HPLC (C-18) with gradient elution [MeCN–H₂O v/v, 80 : 20 to 20 : 80, over 27 min, flow rate = 3 mL min⁻¹].

HPLC (C-18) with gradient elution [MeCN–H₂O v/v, 10 : 90 to 100 : 0, over 27 min, flow rate = 0.8 mL min⁻¹] was used to verify the purity of compounds.

2.8 Evaluation of antimicrobial and antifungal activities of the new compound

To assess antimicrobial activity, the minimum inhibitory concentration (MIC) method was used against a series of bacterial strains in accordance with Clinical and Laboratory Standards Institute (CLSI) recommendations.^{26,27} Briefly, serial two-fold dilutions of each test sample were prepared in sterile broth LB or PDB within a 96-well microplate, yielding a final concentration range of 0.125–200 µg mL⁻¹. Ampicillin sodium and amphotericin B were employed as positive controls for antibacterial and antifungal activities, respectively. The inoculated microplate was then incubated at 37 °C or 30 °C under aerobic conditions for 24 h. After incubation, the MIC was

defined as the lowest concentration of the test sample that elicited complete inhibition. The MIC was analyzed by measuring the absorbance at 600 nm or 450 nm using a microplate reader.²⁷ Experiments were performed in triplicate to ensure data reproducibility. The compound was tested for efficacy against *E. coli*, *S. aureus*, and *B. berengeriana*.

2.9 Antibacterial mechanism

Compound 1 was mixed with logarithmic-phase *E. coli* at 2 × MIC (37.0 µg mL⁻¹). Following 30 min of co-cultivation, the mixture was centrifuged to remove the supernatant, washed thrice with PBS, and fixed in 2 mL of 2.5% glutaraldehyde at 4 °C for 12 h. After dehydration using ethanol solutions (30%, 50%, 70%, 80%, 90%, 95%, and 100%, v/v), samples were subjected to critical point drying with liquid carbon dioxide to preserve bacterial ultrastructure. Dried samples were mounted on aluminum stubs and sputter-coated with a thin layer of gold to enhance electrical conductivity. Prepared samples were observed and imaged under a scanning electron microscope (Hitachi SU8010) at an acceleration voltage of 5 kV.²⁸



Table 2 Differential characteristics of strain Rer75 and its closely related strains^a

| Characteristic | 1 | 2 | 3 | 4 |
|---------------------------------------|-------------------|-----------------------|---------------|----------------------|
| Morphology | | | | |
| Color of clone on ISP 3 | Grey white | ND | Pale yellow | White |
| Color of clone on ISP 5 | Pale yellow | ND | White | Pale greenish yellow |
| Color of clone on ISP 7 | Signal white | Light yellowish brown | Grayish green | White |
| Soluble pigments on ISP 7 | Light olive green | — | — | — |
| Growth temperature (°C) | 20–40 | 24–40 | 20–37 | 10–37 |
| pH 9 | — | + | + | + |
| 8% NaCl (w/v, %) | — | + | — | + |
| Hydrolysis of cellulase | — | + | — | — |
| Coagulation and peptonization of milk | + | ND | — | + |
| Carbon source utilization | | | | |
| Myo-inositol | + | + | — | — |
| Raffinose | + | + | — | + |
| L-rhamnose | + | + | + | + |
| D-mannitol | + | + | — | — |
| Genome size (bp) | 10 474 412 | 9 645 891 | 11 008 137 | 11 030 030 |
| GC content | 71.42 | 71.88 | 71.34 | 67.58 |
| No. of contigs | 1 | 2 | 887 | 783 |
| No. of CDSs | 9191 | 8002 | 9182 | 9256 |
| No. of rRNA genes | 18 | 21 | 6 | 5 |
| No. of tRNA genes | 72 | 68 | 67 | 62 |

^a Strains: 1. Rer75; 2. *Streptomyces rimosus* subsp. *rimosus* NBRC 12907^T; 3. *Streptomyces botrytidirepellens* NEAU-LD23^T; 4. *Streptomyces himastatinicus* ATCC 53653^T.

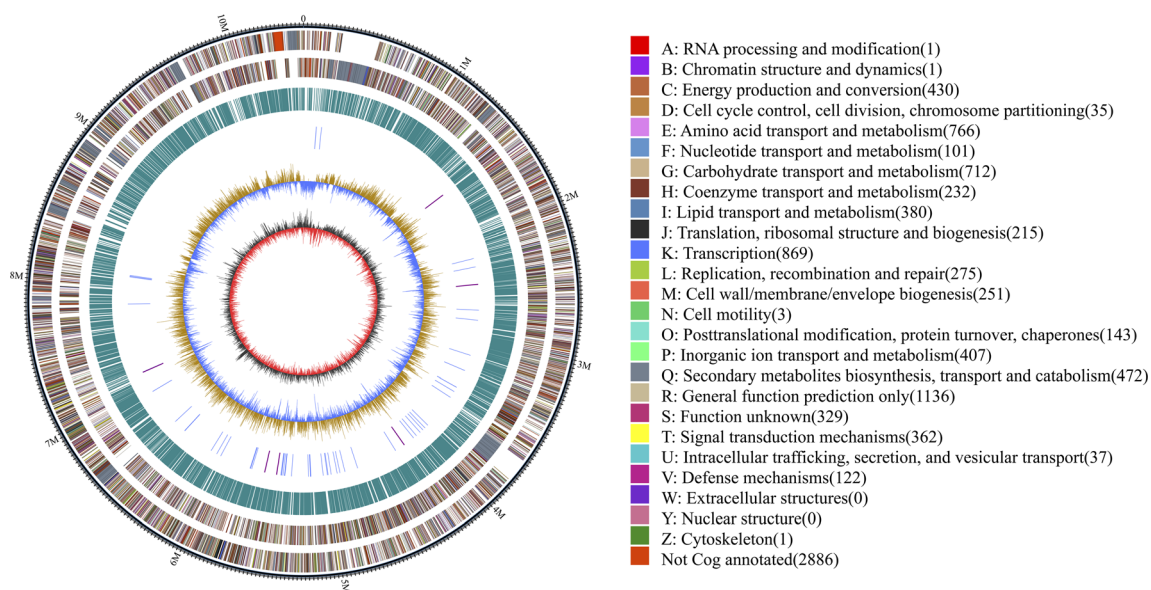


Fig. 5 Genome map of strain Rer75. The outermost circle represents the genome size. The second and third circles depict genes on the positive and negative strands of the genome, respectively, with different colors indicating various COG functional classifications. The fourth circle displays repeat sequences, while the fifth indicates tRNA (blue) and rRNA (purple). The sixth circle represents GC content, and the innermost circle shows the GC skew. The letters A–Z correspond to the functional classification of CDS genes in the chromosome.

2.10 Statistical analyses

Antimicrobial assays were performed thrice. Statistical analyses were performed using SPSS 27.0. Results are the mean \pm standard error of the mean.

3 Results

3.1 Inhibition effect of Rer75 upon plant disease fungi

Strain Rer75 displayed potent broad-spectrum antifungal activity against six pathogenic fungi (Fig. 1A), with percent inhibition values of 43.3–78.3% (Fig. 1B). The highest value



(78.3 ± 2.74%) was against *E. turcicum* (Fig. 1). This indicated that Rer75 produced broad-spectrum antifungal compounds that inhibited the mycelial growth of multiple pathogens, highlighting its research potential.

3.2 Characterization of strain Rer75

Strain Rer75 was a Gram-positive, aerobic, non-motile actinobacterium forming branched substrate hyphae and aerial mycelia that differentiated into flexuous spore chains with

smooth cylindrical spores (0.4–1 μm × 0.1–0.3 μm) (Fig. S2). It grew optimally on ISP 3, ISP 6, ISP 7 and Bennett's agar, forming white-to-grey colonies (Fig. S3). Optimal growth occurred at pH 7.0 (pH range = 6–8) and 28 °C (temperature range = 20–40 °C). Growth was observed at 0–4% NaCl, with the highest yield at 0% salinity. Physiologically, Rer75 was positive for protease, starch hydrolysis and catalase, but negative for tween 20/40/80 hydrolysis, cellulose decomposition, urease, H₂S production and nitrate reduction. It utilized D-glucose, D-xylose, sucrose, D-mannose, meso-inositol, L-rhamnose, D-fructose, D-sorbitol, L-arabinose, D-galactose, lactose, mannitol, D-raffinose and D-maltose (not D-ribose) as sole carbon sources. It utilized L-alanine, L-asparagine, L-aspartic acid, creatine, L-glutamic acid, L-glutamine, L-proline, L-threonine and L-tyrosine (not D-arginine or L-serine) as sole nitrogen sources. The cell wall contained LL-diaminopimelic acid as the major component. Whole-cell sugars were galactose, mannose and rhamnose. Its phospholipid profile included diphosphatidylglycerol, phosphatidylmethylethanolamine, phosphatidylethanolamine and phosphatidylinositol (phospholipid type II sensu) (Fig. S4). The major menaquinones were MK-8 (15.2%), MK-8(H₂) (18.6%), MK-9(H₆) (29.6%) and MK-9(H₈) (36.7%).

3.3 Phylogenetic and genomic analyses

The 16 S rRNA sequence of Rer75 (1527 bp; GenBank accession: OQ073463) showed the highest similarity (99.88%) to *Streptomyces rimosus* subsp. *rimosus* ATCC 10970^T.²⁹ Phylogenetic trees based on 16 S rRNA showed that Rer75 formed an independent branch, with its closest strains being *Streptomyces himastatinicus* ATCC 53653^T (97.93%),³⁰ and *Streptomyces botrytidirepellens* NEAU-LD23^T (98.60%)³¹ (Fig. 2). Whole-genome phylogenetic

Table 3 Genomic features of Rer75

| Description | Statistic |
|---|------------|
| Genome size (bp) | 10 474 412 |
| No. of contigs | 1 |
| Plasmids | 0 |
| G + C content (%) | 71.42 |
| Total number of CDSs | 9191 |
| rRNA genes | 18 |
| tRNA genes | 72 |
| Other ncRNA | 145 |
| Pseudo genes (total) | 3 |
| CRISPR region | 58 |
| Genomic_island | 28 |
| Prophage_region | 6 |
| Genes assigned to COG | 5761 |
| Genes assigned to KEGG | 2197 |
| Genes assigned to Pfam | 7027 |
| Gene entries assigned to CAZy | 430 |
| Gene entries assigned to ARDB | 2 |
| Features assigned by RAST | 2134 |
| Secondary metabolite gene clusters BGCs | 40 |

Table 4 Number of genes associated with COG function class in genes and their relative abundance

| Function class | COG function class | Number of genes | Percentage (%) |
|----------------|---|-----------------|----------------|
| A | RNA processing and modification | 1 | 0.01 |
| B | Chromatin structure and dynamics | 1 | 0.01 |
| C | Energy production and conversion | 430 | 5.91 |
| D | Cell cycle control, cell division, chromosome partitioning | 35 | 0.48 |
| E | Amino acid transport and metabolism | 766 | 10.52 |
| F | Nucleotide transport and metabolism | 101 | 1.39 |
| G | Carbohydrate transport and metabolism | 712 | 9.78 |
| H | Coenzyme transport and metabolism | 232 | 3.19 |
| I | Lipid transport and metabolism | 380 | 5.22 |
| J | Translation, ribosomal structure and biogenesis | 215 | 2.95 |
| K | Transcription | 869 | 11.94 |
| L | Replication, recombination and repair | 275 | 3.78 |
| M | Cell wall/membrane/envelope biogenesis | 251 | 3.45 |
| N | Cell motility | 3 | 0.04 |
| O | Posttranslational modification, protein turnover, chaperones | 143 | 1.96 |
| P | Inorganic ion transport and metabolism | 407 | 5.59 |
| Q | Secondary metabolites biosynthesis, transport and catabolism | 472 | 6.48 |
| R | General function prediction only | 1136 | 15.6 |
| S | Function unknown | 329 | 4.52 |
| T | Signal transduction mechanism | 362 | 4.97 |
| U | Intracellular trafficking, secretion, and vesicular transport | 37 | 0.51 |
| V | Defense mechanisms | 122 | 1.68 |
| Z | Cytoskeleton | 1 | 0.01 |



analyses demonstrated that strain Rer75 formed an independent lineage in close association with *S. botrytidirepellens* NEAU-LD23^T (Fig. 3). However, dDDH and ANI values between Rer75 and its closest relatives were below the recommended thresholds dDDH (<70%) and ANI (<95%) for species delineation^{32,33} (Fig. 3 and 4). Besides, the genomic information and phenotypic differences further distinguished it from related strains (Table 2). These results confirmed Rer75 to be a novel species, for which the name “*Streptomyces rehmanniae*” was proposed.

The complete circular genome was 10.47 Mb with a GC content of 71.42% (Fig. 5) (GenBank accession: CP058693). It encoded 9191 CDSs, 18 rRNAs, 72 tRNAs, and 145 other RNAs (Table 3). COG and RAST analyses indicated abundant genes for

general function, transcription, and the metabolism of amino acids and carbohydrates (Table 4 and Fig. S5). AntiSMASH analyses predicted 40 BGCs for diverse secondary metabolites, including polyketides (PKS), non-ribosomal peptides (NRPS), terpenes, post-translationally modified peptide products (RiPP-like), *Trans*-AT PKS, heterocyst glycolipid synthase-like PKS (hglE-KS) and others (Table 5).

3.4 A nigericin-like gene cluster is essential for antibacterial activity of Rer75

To verify the function of nigericin-like gene cluster no. 37 (Fig. 6A), expression of its core biosynthetic gene *ctg_8048* was repressed. The repression expression vector pSETddCpf1-R8048

Table 5 Biosynthetic gene clusters for the secondary metabolites in strain Rer75

| Cluster no. | AntiSMASH type descriptor | Length (bp) | Predicted products (%) | MIBiG-ID |
|-------------|--|-------------|--|------------|
| 1 | Terpene, T1PKS, pyrrolidine, butyrolactone | 371 697 | X-14547 (30%) | BGC0000079 |
| 2 | Other | 41 382 | A-503083 A, B, E, F (9%) | BGC0000288 |
| 3 | NRPS | 49 075 | Coelichelin (90%) | BGC0000325 |
| 4 | T1PKS | 43 523 | Meilingmycin (8%) | BGC0000207 |
| 5 | Redox-cofactor | 22 094 | Lankacidin C (13%) | BGC0000518 |
| 6 | Butyrolactone | 10 013 | — | — |
| 7 | NRPS | 78 474 | Dechlorocuracomycin (8%) | BGC0000389 |
| 8 | Terpene | 24 241 | Isorenieratene (71%) | BGC0000664 |
| 9 | Terpene | 19 121 | Pristinol (100%) | BGC0001746 |
| 10 | Lanthipeptide-class-iii | 20 412 | — | — |
| 11 | NRPS | 44 820 | Rifamorpholine A–E (3%) | BGC0000375 |
| 12 | Siderophore | 11 802 | — | — |
| 13 | Ectoioine | 10 404 | Ectoioine (100%) | BGC0000853 |
| 14 | Phenazine | 20 488 | 5-Acetyl/5-(2-hydroxyacetyl) –5,10-dihydrophenazine-1-carboxylic acid/endophenazine A1, F, G (30%) | BGC0000936 |
| 15 | NRPS-like, T1PKS | 209 530 | Mediomycin A (68%) | BGC0001932 |
| 16 | RRE-containing | 21 531 | Granaticin (10%) | BGC0001514 |
| 17 | Arylpolyene, ladderane | 42 391 | Atratamycin (34%) | BGC0001343 |
| 18 | NRPS | 43 358 | Ochronotic pigment (75%) | BGC0001615 |
| 19 | Terpene | 21 460 | Geosmin (100%) | BGC0001181 |
| 20 | Lasso peptide | 22 565 | SSV-2083 (18%) | BGC0001779 |
| 21 | Siderophore | 11 306 | Desferrioxamin B (100%) | BGC0001478 |
| 22 | Lanthipeptide-class-iii | 22 645 | Catenulipeptin (60%) | BGC0000553 |
| 23 | NRPS-like | 41 523 | Echoside A–E (82%) | BGC0000340 |
| 24 | T1PKS, PKS-like | 114 768 | Incednine (17%) | BGC0000068 |
| 25 | Siderophore | 12 366 | — | — |
| 26 | RiPP-like | 8677 | — | — |
| 27 | T2PKS | 72 524 | Spore pigment (83%) | BGC0000272 |
| 28 | transAT-PKS | 61 483 | 9-Methylstreptimidone (77%) | BGC0000171 |
| 29 | Terpene | 26 146 | Hopene (69%) | BGC0000663 |
| 30 | T3PKS, transAT-PKS, NRPS, T1PKS | 110 392 | Phthoxazolin (9%) | BGC0000282 |
| 31 | T1PKS | 65 414 | Aculeximycin (14%) | BGC0000041 |
| 32 | NRPS, T1PKS, lanthipeptide-class-ii | 64 583 | Guadinomine (7%) | BGC0001579 |
| 33 | T1PKS, NRPS, PKS-like, butyrolactone | 202 119 | BE-14106 (64%) | BGC0000848 |
| 34 | hglE-KS, T1PKS | 51 053 | — | — |
| 35 | RiPP-like | 10 224 | — | — |
| 36 | NAPAA | 33 950 | Phthoxazolin (6%) | BGC0000674 |
| 37 | T1PKS | 125 835 | Nigericin (94%) | BGC0000114 |
| 38 | NRPS-like, terpene | 49 318 | Livipeptin (100%) | BGC0001181 |
| 39 | T1PKS, NRPS-like, terpene | 43 431 | 2-Methylisoborneol (100%) | BGC0000658 |
| 40 | T1PKS, terpene | 110 096 | Spectinabilin/orinocin/SNF4435C–D (36%) | BGC0000674 |



was constructed (Fig. 6B), and conjugal transfer was performed to obtain Rer75-R8045 mutants. Verification *via* ampicillin resistance gene amplification showed no corresponding amplicon in the wild-type strain (lacking this resistance gene), while a specific 570-bp band was detected in the transconjugant (Fig. 6C). The original strain and repression strain were fermented in H9 medium, followed by an antibacterial assay. A plate confrontation assay was used to verify the changes in the antifungal activity of the mutant strain. Results indicated that the antibacterial activity of the repression strain decreased by nearly 50%, but with no changes in the antifungal activity (Fig. 6D), confirming that nigericin-like gene cluster no. 37 in Rer75 was responsible for the biosynthesis of antibacterial metabolites.

3.5 Optimization of the fermentation medium

Streptomyces species produce different secondary metabolites depending on the culture medium used. Antimicrobial activity

screening of extracts from eight different media revealed that the H9 medium yielded the strongest activity against *E. coli*, *S. aureus*, and *B. berengeriana*, making it the chosen medium for large-scale compound isolation (Fig. 7).

3.6 Structure elucidation

Seven compounds were isolated from the H9 fermentation culture of Rer75 (Fig. 8). Compound 1 was obtained as a colorless oil and was identified as a pure compound by HPLC (Fig. S6). Its $[M + H]^+$ ion was observed at m/z 405.2046 (calcd. m/z 405.2046) using HRESIMS (Fig. S7), allowing the determination of its molecular formula as $C_{19}H_{33}O_9$. The planar structure of 1 was established by comprehensive analyses of 1D and 2D NMR data. The 1H NMR spectrum (Table 6 and Fig. S8–S10) showed characteristic signals for two olefinic protons [δ_H 5.88 (dt, $J = 15.6, 1.5$ Hz, H-2); 6.89 (dt, $J = 15.3, 7.5$ Hz, H-3)], four methoxy groups as singlets (δ_H 3.65, 3.66, 3.72, 3.74), and two

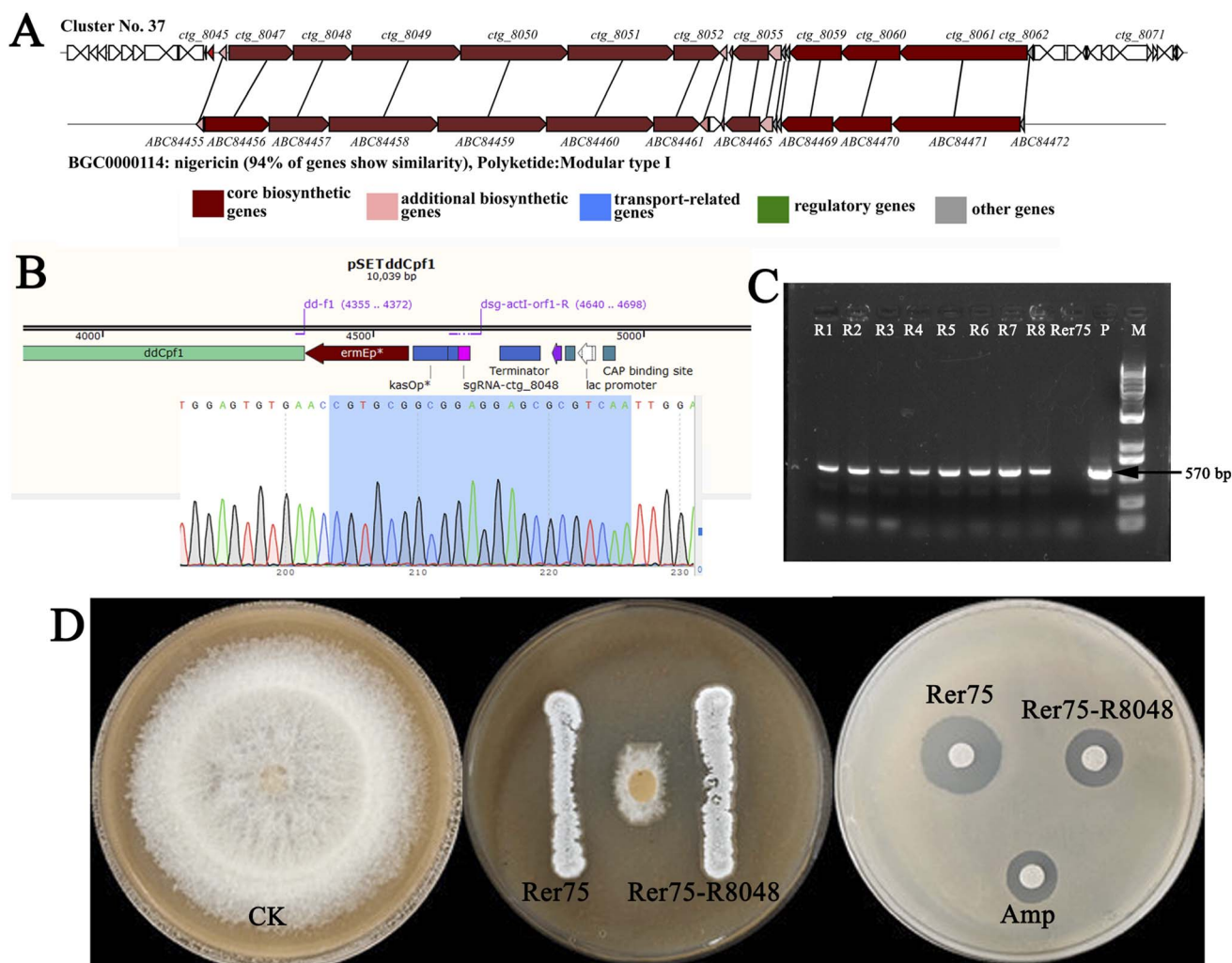


Fig. 6 Relationship between the nigericin-like gene cluster and antibacterial activity of metabolites from strain Rer75. (A) MIBiG comparison of biosynthetic gene cluster by region-to-region analysis type. (B) Construction of the *ctg_8048*-inhibitory plasmid based on pSETddCpf1. (C) PCR amplification of the ampicillin resistance gene; R1–R8: gene-inhibited strains obtained *via* conjugation transfer; P: plasmid pSETddCpf1-R8048; M: marker. (D) Antimicrobial activity between the R8048 mutant strain and the wild-type strain Rer75. CK: *F. graminearum* Schw grown on V8 agar.



methyl groups as doublets (δ_{H} 1.23, 1.26). ^{13}C NMR and DEPT spectra (Fig. S11–S13) displayed 19 carbon resonances corresponding to two sp^2 carbons (δ_{C} 124.3, 147.6), two sp^3 methyl groups (δ_{C} 16.3, 17.2), four sp^3 methylene groups (δ_{C} 28.6, 32.0, 37.5, 38.8), three sp^3 methine groups (δ_{C} 32.8, 81.5, 81.7), one sp^3 quaternary carbon (δ_{C} 106.4), three carbonyl carbons (δ_{C} 168.3, 174.2, 175.4), and four methoxy groups (δ_{C} 52.0, 52.1, 52.2, 52.9). 1D NMR data indicated a structure related to the known compound *rel-4-Ethyl-1,5-dimethyl (1E,4R,5S)-3,3-dimethoxy-1-heptene-1,4,5-tricarboxylate*.³⁴ ^1H – ^1H COSY and HMBC correlations are shown in Fig. 9. The ^1H – ^1H COSY spectrum (Fig. S14) revealed three spin systems, H-2/H-3/H₂-4, H-5/H₂-6/H₂-7, and H₃-1'/H-2'/H-3'/H₃-4', corresponding to fragments I, II, and III, respectively (Fig. 9). The key HMBC correlations (Fig. S15) from H₃-C-b (δ_{H} 3.72) and H-3 (δ_{H} 6.89) to the carbonyl carbon C-1 (δ_{C} 168.3), from H₃-C-a (δ_{H} 3.65) and

H₂-1'' (δ_{H} 2.39) to C-2'' (δ_{C} 174.2), from H₂-1'' (δ_{H} 2.39) and H₂-4 (δ_{H} 2.31) to C-5 (δ_{C} 32.8), from H₃-C-c (δ_{H} 3.74), H₃-C-d (δ_{H} 3.66), H-2' (δ_{H} 3.86), and H₂-7 (δ_{H} 2.18) to C-9 (δ_{C} 175.4), and from H₂-6 (δ_{H} 2.4) and H₂-7 (δ_{H} 2.18) to the quaternary carbon C-8 (δ_{C} 106.4) connected these fragments and established the planar structure. Based on the spectroscopic data, the structure of compound **1** was elucidated to be dimethyl (*E*)-8-[(3-hydroxybutan-2-yl)oxy]-8-methoxy-5-(2-methoxy-2-oxoethyl) non-2-enedioate, representing a new unsaturated hydroxy ester (Fig. 9). Compounds **2**–**7** were identified as 3,4-bis(*S*)-2-ethylhexyl phthalate (**2**),³⁵ *N*-(4-methoxyphenethyl) acetamide (**3**),³⁶ 4-aminobutanoic acid (**4**),³⁷ piperidin-2-one (**5**),³⁸ *N*-(4-ethylphenethyl) acetamide (**6**)³⁹ and methyl 2-(4-hydroxyphenyl) acetate (**7**)⁴⁰ by comparing their spectroscopic data with the literature (Fig. 8).

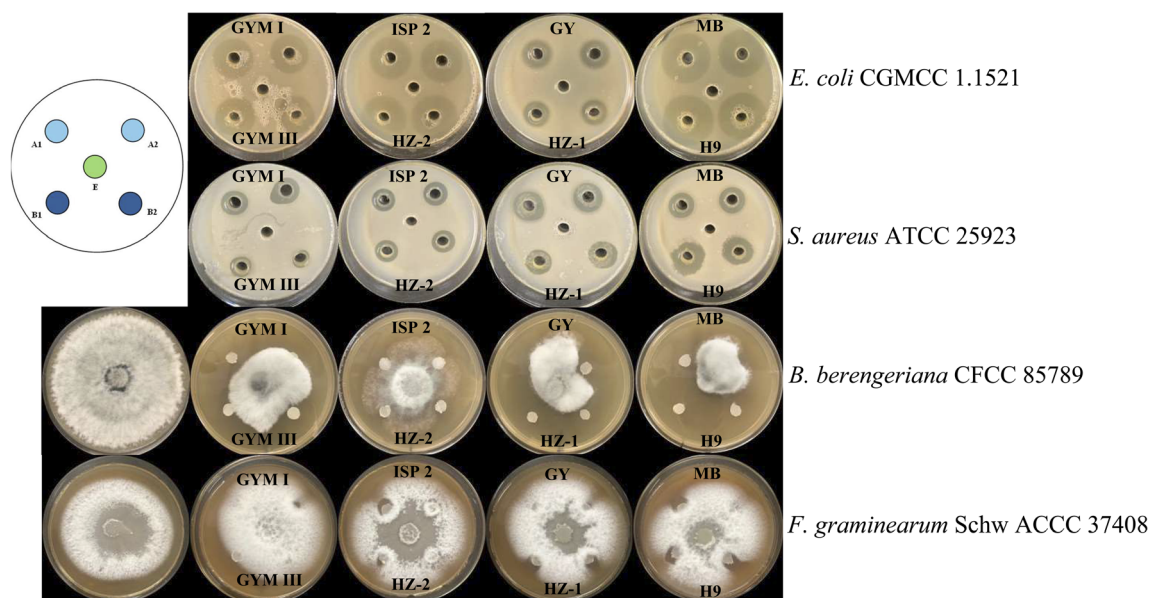


Fig. 7 Antimicrobial activities of extracts from different fermentations of Rer75. A1 and B1: supernatant extracts; A2 and B2: precipitation extract; E: different pathogens.

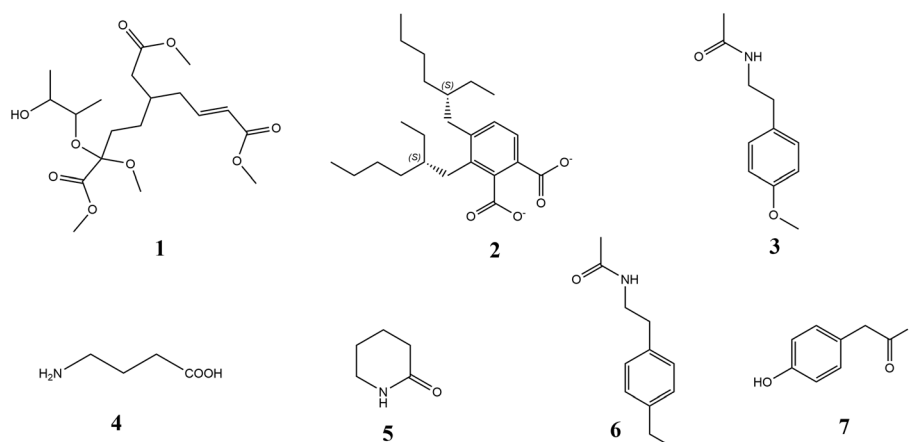


Fig. 8 Chemical structures of compounds **1**–**7** isolated from *Streptomyces rehmianae* Rer75.



Table 6 ^1H and ^{13}C NMR data of compound 1 in MeOD

| Position | δ_{C} | δ_{H} (int., mult., J in Hz) |
|---------------------|---------------------|--|
| 1 -C=O | 168.3 | — |
| 2 | 124.3 | 5.88 (1H, dt, 15.6, 1.5) |
| 3 | 147.6 | 6.89 (1H, dt, 15.3, 7.5) |
| 4 | 37.5 | 2.31 (2H, ddd, 8.0, 6.6, 1.5) |
| 5 | 32.8 | 2.50 (1H, dt, 13.3, 6.8) |
| 6 | 28.6 | 2.4 (2H, m) |
| 7 | 32.0 | 2.18 (2H, m) |
| 8 | 106.4 | — |
| 9 -C=O | 175.4 | — |
| 1' | 17.2 | 1.23 (3H, d, 6.1) |
| 2' -C-O- | 81.7 | 3.86 (1H, dd, $J = 8.4, 6.0$) |
| 3' -C-OH | 81.5 | 3.66 (1H, m) |
| 4' | 16.3 | 1.26 (3H, d, 6.0) |
| 1'' | 38.8 | 2.39 (2H, m) |
| 2'' -C=O | 174.2 | — |
| a -OCH ₃ | 52.1 | 3.65 (3H, s) |
| b -OCH ₃ | 52.2 | 3.72 (3H, s) |
| c -OCH ₃ | 52.9 | 3.74 (3H, s) |
| d -OCH ₃ | 52.0 | 3.66 (3H, s) |

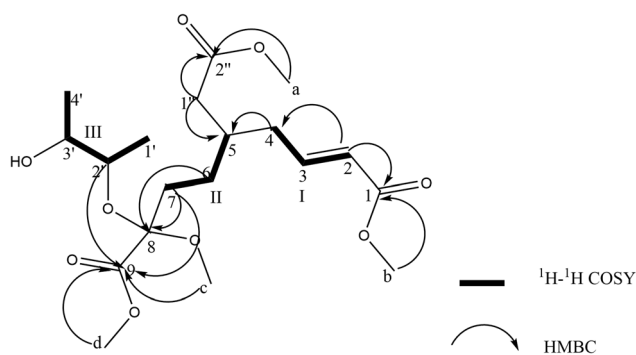


Fig. 9 2D nuclear magnetic resonance correlations of compound 4.

3.7 Biological activity

The new compound 1 exhibited moderate antimicrobial activity against *E. coli* ($\text{MIC} = 18.3 \pm 2.3 \mu\text{g mL}^{-1}$) and *S. aureus* ($\text{MIC} = 35.8 \pm 3.6 \mu\text{g mL}^{-1}$) compared with ampicillin sodium (9.67 ± 2.84 and $1.35 \pm 4.1 \mu\text{g mL}^{-1}$) but showed no activity against the fungal pathogen *B. berengeriana* (Table 7).

3.8 Antibacterial mechanism of compound 1

As shown in Fig. 10A, in the absence of compound treatment, *E. coli* exhibited a normal morphology with intact cell walls and

Table 7 Antibacterial activity of compound 1

| Compounds | MIC ($\mu\text{g mL}^{-1}$) | | |
|-------------------|-------------------------------|-----------------------------|-----------------------------------|
| | <i>E. coli</i> CGMCC 1.1521 | <i>S. aureus</i> ATCC 25923 | <i>B. berengeriana</i> CFCC 85789 |
| 1 | 18.3 ± 2.3 | 35.8 ± 3.6 | >200.0 |
| Ampicillin sodium | 9.67 ± 2.84 | 1.35 ± 4.1 | — |
| Amphotericin B | — | — | 4.23 ± 0.75 |

clear boundaries. In contrast, when treated with compound 1 at a concentration of $2 \times \text{MIC}$ ($37.0 \mu\text{g mL}^{-1}$), obvious morphological damages were observed, such as a fractured cell wall and membranes, released intracellular contents, and cells presented as empty shells (Fig. 10B). These results clearly indicated that the new compound exerted a bactericidal effect by damaging the cell walls and cell membranes of *E. coli* (Fig. 10).

4 Discussion

Microbial resistance to antibiotics is an ancient and naturally occurring phenomenon. The dangers of AMR must be addressed to avoid escalating threats to public health.¹ Screening for new antimicrobials with strong activity is important. Antimicrobial compounds are produced by microbes, especially actinomycetes such as *Streptomyces*, *Nocardia* and *Micromonospora* species.⁴¹ Among them, *Streptomyces* species exhibit remarkable adaptability across diverse ecological niches, making them a subject of extensive investigation.⁴² Daptomycin, a cyclic lipopeptide antibiotic, derived from *Streptomyces roseosporus*, exerts its bactericidal activity through inhibition of critical cellular processes, including protein, DNA and RNA synthesis, which ultimately cause bacterial cell death.⁴³ Daptomycin has been approved for the treatment of complicated skin and skin structure infections (cSSSI) in the USA.⁴³ Furthermore, various secondary metabolites derived from *Streptomyces* species, including jinggangmycin,⁴⁴ zhongshengmycin,⁴⁵ and avermectin,⁴⁶ have been commercialized as biopesticides in agriculture. During the investigation of rhizosphere microorganisms in *R. glutinosa*, a strain designated “Rer75” with strong antifungal activity was isolated. Polyphasic taxonomic characterization revealed strain Rer75 to be a newly discovered *Streptomyces* species. Then, the genome of strain Rer75 was sequenced for detailed analyses. Subsequent optimization of culture conditions and compounds isolation were carried out to obtain bioactive metabolites exhibiting antimicrobial properties.

With the rapid development of biological information technology, genomics has reached a stage where it may be used in prokaryotic taxonomic classification. Digital DNA–DNA hybridization (dDDH), based on genomic data, is a “gold standard” for bacterial species identification.⁴⁷ It directly reflects overall genomic DNA hybridization homology and serves as the core traditional criterion for prokaryotic species demarcation. Therefore, although the ANI value (94.94%) between Rer75 and *S. botrytidirepellens* NEAU-LD23^T fell within the borderline range (95–96%) for species demarcation, strain Rer75 was recognized as a novel species of the genus *Streptomyces* because its dDDH value (65.60%) was significantly below the 70% threshold for species delineation (Fig. 3 and 4). In addition, notable morphological differences were observed between Rer75, *S. botrytidirepellens* NEAU-LD23^T and *S. himastatinicus* ATCC 53653^T. For instance, strain Rer75 produced a pale olive-green pigment on ISP 7 medium, whereas strains NEAU-LD23^T and ATCC 53653^T did not; Rer75 exhibited a grey colour on ISP 3 medium, while strains NEAU-LD23^T and ATCC 53653^T were pale-yellow and white, respectively (Table 2).^{30,31} Collectively,



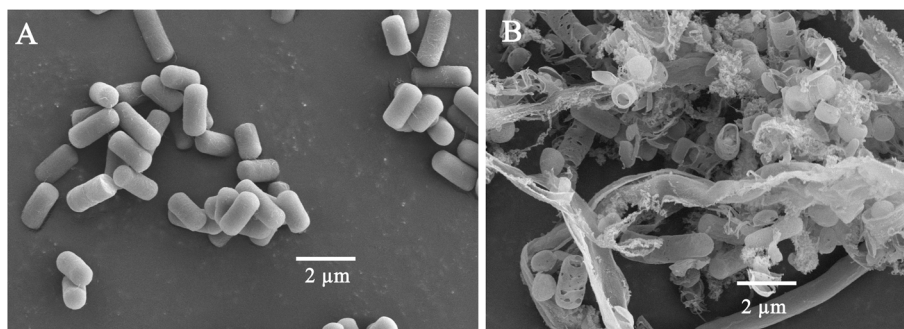


Fig. 10 SEM of *E. coli* and *E. coli* treated with compound 1. (A) SEM of *E. coli*. (B) SEM of *E. coli* treated with $37 \mu\text{g mL}^{-1}$ of compound 1.

with the other differences listed in Table 2, strains Rer75, NEAU-LD23^T and ATCC 53653^T represent distinctly different *Streptomyces* species, demonstrating that Rer75 is a novel species of genus *Streptomyces* proposed as *Streptomyces rehmanniae*.

To investigate the antibacterial-active components of strain Rer75, H9 medium was selected for large-scale fermentation to isolate antimicrobial compounds. Seven compounds were obtained from the medium, and compound 1 was a new compound. As shown in Fig. 8, compound 1 possessed a highly flexible linear chain with multiple chiral carbon centers, including C5, C8, C2' and C3'. This structural feature led to significant conformational mobility, making it difficult to obtain clear through-space correlations from nuclear magnetic resonance (NMR) techniques such as NOESY/ROESY, which are commonly used to deduce relative stereochemistry.⁴⁸ Furthermore, the literature was searched, and no structurally analogous compounds with reported stereochemistry were found. Nevertheless, the structural characterization presented was otherwise considered comprehensive and reliable, having been firmly established based on detailed NMR (¹H, ¹³C, DEPT, HSQC, HMBC) and MS data.

It has been reported that the bioactive compounds produced by *Streptomyces* are derived from BGCs, with the enzymes being arranged in close proximity within bacterial genomes.⁴⁹ As depicted in Fig. 11, a putative biosynthetic pathway was proposed for compound 1, which is presumably synthesized by type-I polyketide synthase (T1PKS). The biosynthetic pathway is similar to that for spectinabilin.⁵⁰ Through comprehensive mining of the genome of Rer75, 14 distinct T1PKS gene clusters

were identified (Table 5). Despite in-depth bioinformatics analysis of these gene clusters, no suitable T1PKS gene cluster whose modular organization and domain composition could fully account for compound 1 was identified because of its specific carbon chain length, methylation pattern, and the presence of hydroxyl groups and double bonds. Besides, compound 1 may be a product of a hybrid pathway combined with cytochrome P450 oxidases, glycosyltransferases, or methyltransferases encoded outside the core PKS cluster that account for its unique structural features, making it difficult to link the final product to the core PKS cluster *via* bioinformatics analysis alone.

A deeper understanding of the BGCs in *Streptomyces* species will therefore be more useful for the research and applications of active compounds in *Streptomyces* species. For example, strain *Streptomyces* sp. S4–7, which encodes 35 BGCs for producing putative antimicrobial agents, originally showed suppression against *Fusarium* wilt. Also, through genome analysis, a novel thiopeptide was purified and shown to have potent inhibitory activity against fungal cell wall biogenesis in *Fusarium* species.⁵¹ Thus, the application of *in silico* biosynthetic predictions from genome mining data is usually employed for screening promising *Streptomyces* species in nature. Strain Rer75 contains 40 BGCs in the genome, and 33 clusters were similar to BGCs with known functions (Table 5). Six gene clusters contained 100% similarity with the known cluster that could synthesize pristinol, ectoine, geosmin, desferrioxamin B, livipeptin and 2-methylisoborneol in *Streptomyces* strains (Table 5). Besides, five BGCs were expected to produce known compounds with identical

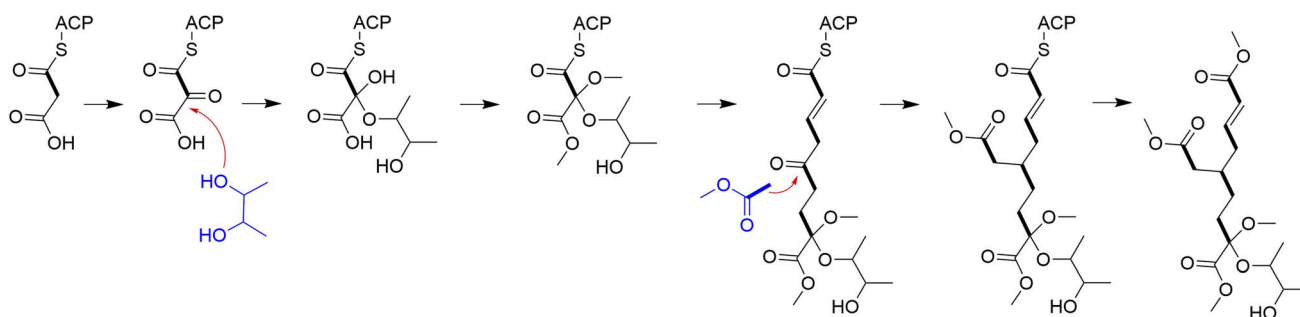


Fig. 11 Putative biosynthetic pathway of compound 1.

predicted functions at high levels of similarity (77–94%) (Table 5). Nigericin, an H⁺, K⁺ and Pb²⁺ ionophore, exhibited promising activity against various types of cancer. Treatment of cancer cells with nigericin may offer a novel therapeutic strategy and potential for future clinical translation.⁵² Recently, Zhu *et al.* revealed that nigericin also exhibits potent antibacterial activity.⁵³ In the genome of Rer75, a T1PKS gene cluster no. 37 (*ctg_8033–ctg_8077*), which had high similarity (94%) to nigericin, was found. Except for the additional biosynthetic gene *ABC84463*, all the genes of nigericin BGCs (Fig. 6 and Table S2) were found in the genome of Rer75, and the MIBiG comparison with region-to-region analysis is shown in Fig. 6A. Collectively, repression of the core gene *ctg_8048* in cluster no. 37 identified the biological importance of the cluster in the synthesis of antibacterial secondary metabolites (Fig. 6), laying a solid foundation for in-depth mechanistic and structural investigations. Further work will therefore focus on elucidating the precise chemical structure of the metabolite encoded by cluster no. 37 and deciphering its underlying molecular mechanism of antibacterial action. As shown in Fig. 6D, antibacterial activity was not completely abrogated upon inhibition of the nigericin-like gene cluster, indicating the presence of other antibacterial bioactive metabolites awaiting further exploration. In addition, *Streptomyces* species have a rich repertoire of secondary metabolites, yet these natural products are often hampered by low yields and the transcriptional silencing of numerous BGCs under standard laboratory cultivation conditions.⁵⁴ To address these limitations, genome-guided mining approaches will be prioritized in subsequent studies to uncover novel bioactive secondary metabolites with potential antimicrobial properties from investigated strains.

Author contributions

All authors contributed to the study conception and design. Hairong He and Pengqiang Du conceived and wrote this work. Hairong He isolated microbes. Tong Wang and Jiaqi Li carried out tests on antifungal activities, isolation of compounds, and antimicrobial activity. Hairong He, Zhenzhu Zhao, Zhaoxu Ma analyzed genome data. Chen Sun verified the function of gene cluster no. 37. Hairong He, Pengqiang Du and Xiaoke Zheng revised the manuscript.

Conflicts of interest

The authors have no relevant financial or non-financial interests to disclose.

Data availability

NCBI gene bank *Streptomyces* sp. strain Rer75 16 S ribosomal RNA gene, partial sequence (nucleotide): NCBI, <https://www.ncbi.nlm.nih.gov/nuccore/OQ073463.1>; strain Rer75 chromosome (nucleotide): NCBI, <https://www.ncbi.nlm.nih.gov/nuccore/CP058693.1>.

Supplementary information (SI) is available. See DOI: <https://doi.org/10.1039/d5ra07947k>.

Acknowledgements

This work was supported by National Natural Science Foundation of China (“Effect and mechanism of recruitment of the rhizosphere beneficial microorganisms of *Rehmannia glutinosa* in response to plant pathogenic fungi under the stress of ring rot disease”; 32302411); Postdoctoral Foundation of Henan Province (“Study on the rhizosphere microecological regulation mechanism of *Streptomyces* sp. RerS4-mediated resistance to ring rot disease in *Rehmannia glutinosa*”; HN2025061); Natural Science Foundation of Henan (“Research on soil function and microbial ecology in the rhizosphere of *Lonicera japonica* mediated by *Pseudomonas extremorientalis*”; 242301420144); Kunlun Talent High-end Innovation and Entrepreneurship Talent Leading Talent Project of Qinghai Province (2024). We sincerely acknowledge Professor Yinhua Lu from Shanghai Normal University for providing the inhibitory plasmid, and Professor Yanyan Zhang from the Institute of Plant Protection, Chinese Academy of Agricultural Sciences, for offering guidance on the conjugative transfer experiment. Besides, we thank Biomarker Technologies for assisting in the genome sequencing of strain Rer75.

References

- 1 K. W. K. Tang, B. C. Millar and J. E. Moore, Antimicrobial Resistance (AMR), *Br. J. Biomed. Sci.*, 2023, **80**, 11387.
- 2 F. Prestinaci, P. Pezzotti and A. Pantosti, Antimicrobial resistance: a global multifaceted phenomenon, *Pathog. Glob. Health*, 2015, **109**(7), 309–318.
- 3 P. M. Ngegba, G. Cui, M. Z. Khalid, *et al.*, Use of botanical pesticides in agriculture as an alternative to synthetic pesticides, *Agriculture*, 2022, **12**, 600.
- 4 P. Chatterjee and Ü. Niinemets, Improving plant stress resistance by growth-promoting bacteria and evaluating the improvements by volatile emissions, *Plant Soil*, 2022, **476**, 403–419.
- 5 S. A. Asad, Mechanisms of action and biocontrol potential of *Trichoderma* against fungal plant diseases - a review, *Ecol. Complex.*, 2022, **49**, 100978.
- 6 J. Dobrzyński and A. Naziębło, *Paenibacillus* as a biocontrol agent for fungal phytopathogens: Is *P. polymyxa* the only one worth attention?, *Microb. Ecol.*, 2024, **87**(1), 134.
- 7 K. J. Meyer and J. R. Nodwell, *Streptomyces* extracellular vesicles are a broad and permissive antimicrobial packaging and delivery system, *J. Bacteriol.*, 2024, **206**(3), e0032523.
- 8 J. T. Newitt, S. M. M. Prudence, M. I. Hutchings, *et al.*, Biocontrol of cereal crop diseases using Streptomyces, *Pathogens*, 2019, **8**(2), 78.
- 9 J. Li, L. Zhang, G. Yao, *et al.*, Synergistic effect of co-culture rhizosphere *Streptomyces*: A promising strategy to enhance antimicrobial activity and plant growth-promoting function, *Front. Microbiol.*, 2022, **13**, 976484.
- 10 J. W. Li and J. C. Vederas, Drug discovery and natural products: end of an era or an endless frontier?, *Science*, 2009, **325**(5937), 161–165.



- 11 P. Sivalingam, M. Easwaran, D. Ganapathy, *et al.*, Endophytic *Streptomyces*: an underexplored source with potential for novel natural drug discovery and development, *Arch. Microbiol.*, 2024, **206**(11), 442.
- 12 H. R. He, J. R. Huang, Z. Z. Zhao, *et al.*, Whole genome analysis of *Streptomyces* sp. RerS4, a *Rehmannia glutinosa* rhizosphere microbe producing a new lipopeptide, *Heliyon*, 2023, **9**(9), e19543.
- 13 V. González, E. Armijos and A. Garcés-Claver, Fungal endophytes as biocontrol agents against the main soil-borne diseases of melon and watermelon in Spain, *Agronomy*, 2020, **10**, 820.
- 14 S. Kumar, G. Stecher, M. Li, *et al.*, MEGA X: Molecular evolutionary genetics analysis across computing platforms, *Mol. Biol. Evol.*, 2018, **35**, 1547–1549.
- 15 J. P. Meier-Kolthoff and M. Göker, TYGS is an automated high-throughput platform for state-of-the-art genome-based taxonomy, *Nat. Commun.*, 2019, **10**(1), 2182.
- 16 M. Richter, R. Rosselló-Móra, F. O. Glöckner, *et al.*, JSpeciesWS: a web server for prokaryotic species circumscription based on pairwise genome comparison, *Bioinformatics*, 2016, **32**, 929–931.
- 17 T. Wang, C. Gao, H. Chen, *et al.*, *Sphaerisorangium perillae* sp. nov., isolated from the root of *Perilla frutescens* (Linn.) Britt, *Int. J. Syst. Evol. Microbiol.*, 2023, **73**, 005773.
- 18 J. McKerrow, S. Vagg, T. McKinney, *et al.*, A simple HPLC method for analysing diaminopimelic acid diastereomers in cell walls of Gram-positive bacteria, *Lett. Appl. Microbiol.*, 2000, **30**, 178–182.
- 19 D. Minnikin, A. O'donnell, M. Goodfellow, *et al.*, An integrated procedure for the extraction of bacterial isoprenoid quinones and polar lipids, *J. Microbiol. Methods*, 1984, **2**, 233–241.
- 20 S. Koren, B. P. Walenz, K. Berlin, *et al.*, Canu: scalable and accurate long-read assembly via adaptive k-mer weighting and repeat separation, *Genome Res.*, 2017, **27**, 722–736.
- 21 B. J. Walker, T. Abeel, T. Shea, *et al.*, Pilon: an integrated tool for comprehensive microbial variant detection and genome assembly improvement, *PLoS One*, 2014, **9**, e112963.
- 22 D. H. Haft, M. DiCuccio, A. Badretdin, *et al.*, RefSeq: an update on prokaryotic genome annotation and curation, *Nucleic Acids Res.*, 2018, **46**, D851–d860.
- 23 R. K. Aziz, D. Bartels, A. A. Best, *et al.*, The RAST Server: rapid annotations using subsystems technology, *BMC Genom.*, 2008, **9**, 75.
- 24 K. Blin, S. Shaw, A. M. Kloosterman, *et al.*, antiSMASH 6.0: improving cluster detection and comparison capabilities, *Nucleic Acids Res.*, 2021, **49**, w29–w35.
- 25 L. Li, K. K. Wei, G. S. Zheng, *et al.*, CRISPR-Cpf1-assisted multiplex genome editing and transcriptional repression in *Streptomyces*, *Appl. Environ. Microbiol.*, 2018, **84**(18), e0082718.
- 26 H. S. Sader, R. K. Flamm and R. N. Jones, Antimicrobial activity of daptomycin tested against Gram-positive pathogens collected in Europe, Latin America, and selected countries in the Asia-Pacific Region (2011), *Diagn. Microbiol. Infect. Dis.*, 2013, **75**(4), 417–422.
- 27 O. Simonetti, C. Silvestri, D. Arzeni, *et al.*, In vitro activity of the protegrin IB-367 alone and in combination compared with conventional antifungal agents against dermatophytes, *Mycoses*, 2014, **57**(4), 233–239.
- 28 P. C. Braga, M. Culici, D. Ricci, *et al.*, Morphostructural damage and the inhibition of bacterial adhesiveness of *Staphylococcus aureus* and *Moraxella catarrhalis* induced by moxifloxacin, *J. Chemother.*, 2003, **15**(6), 543–550.
- 29 F. E. Pethick, A. C. Macfadyen, Z. Tang, *et al.*, Draft genome sequence of the oxytetracycline-producing bacterium *Streptomyces rimosus* ATCC 10970, *Genome Announc.*, 2013, **1**(2), e0006313.
- 30 Y. Kumar and M. Goodfellow, Five new members of the *Streptomyces violaceusniger* 16S rRNA gene clade: *Streptomyces castelarensis* sp. nov., comb. nov., *Streptomyces himastatinicus* sp. nov., *Streptomyces mordarskii* sp. nov., *Streptomyces rapamycinicus* sp. nov. and *Streptomyces ruanii* sp. nov, *Int. J. Syst. Evol. Microbiol.*, 2008, **58**(6), 1369–1378.
- 31 M. Jiang, X. Xu, J. Song, *et al.*, *Streptomyces botrytidirepellens* sp. nov., a novel actinomycete with antifungal activity against *Botrytis cinerea*, *Int. J. Syst. Evol. Microbiol.*, 2021, **71**(9), 10.
- 32 L. G. Wayne, D. J. Brenner, R. R. Colwell, *et al.*, Report of the ad hoc committee on reconciliation of approaches to bacterial systematics, *Int. J. Syst. Bacteriol.*, 1987, **37**, 463–464.
- 33 J. Chun and F. A. Rainey, Integrating genomics into the taxonomy and systematics of the Bacteria and Archaea, *Int. J. Syst. Evol. Microbiol.*, 2014, **64**, 316–324.
- 34 M. L. Graziano, M. R. Iesce, F. Cermola, *et al.*, Ring-opening reactions of cyclopropanes. Part 7.1 Selenenylation and cyanoselenenylation of ethyl 2,2-dimethoxycyclopropanecarboxylates, *J. Chem. Soc., Perkin Trans. 1*, 2002, 664–668.
- 35 R. S. Xu, K. Yuan, M. W. Yin, *et al.*, Chemical constituents in *Tridax procumbens*, *Chin. Herb. Med.*, 2009, **40**(07), 1015–1018.
- 36 A. E. Wright, G. P. Roth, J. K. Hoffman, *et al.*, Isolation, synthesis, and biological activity of aphrocallistin, an adenine-substituted bromotyramine metabolite from the *Hexactinellida* sponge *Aphrocallistes beatrix*, *J. Nat. Prod.*, 2009, **72**(6), 1178–1183.
- 37 J. Y. Xu, F. Q. Xu, C. H. Kong, *et al.*, Chemical constituents from the roots of *Stephania tetrandra* and their anti-liver fibrosis activity, *Nat. Prod. Res. Dev.*, 2022, **34**(12), 2050–2055.
- 38 H. Wang, H. R. Si, Y. F. Jiao, *et al.*, Chemical constituents from berries of *Brassicarapa* L. ssp. *pekinensis*, *Nat. Prod. Res.*, 2020, **32**, 1343–1347.
- 39 X. L. Yue, Y. Yang, R. Xu, *et al.*, Studies on the secondary metabolites and their cytotoxic activities of an endophytic fungus *Penicillium cinereoatrum* Chalab. JSQ-15 isolated from *Lanmaoa asiatica*, *J. Med. Chem.*, 2023, **33**(05), 367–379.
- 40 A. E. Wright, G. P. Roth, J. K. Hoffman, *et al.*, Isolation, synthesis, and biological activity of aphrocallistin, an adenine-substituted bromotyramine metabolite from the *Hexactinellida* sponge *Aphrocallistes beatrix*, *J. Nat. Prod.*, 2009, **72**(6), 1178–1183.



- 41 K. K. Jakubiec, M. A. Rajnisz, A. Guspiel, *et al.*, Secondary metabolites of actinomycetes and their antibacterial, antifungal and antiviral properties, *Pol. J. Microbiol.*, 2018, **67**(3), 259–272.
- 42 R. T. Magar and J. K. Sohng, Natural products with γ -pyrone scaffold from *Streptomyces*, *Appl. Microbiol. Biotechnol.*, 2024, **108**(1), 471.
- 43 J. N. Steenbergen, J. Alder, G. M. Thorne, *et al.*, Daptomycin: A lipopeptide antibiotic for the treatment of serious gram-positive infections, *J. Antimicrob. Chemother.*, 2005, **55**, 283–288.
- 44 W. Dong, W. J. Wu, C. Y. Song, *et al.*, Jinglyngmycin stimulates reproduction and increases CHCs-dependent desiccation tolerance in *Drosophila melanogaster*, *Pestic. Biochem. Physiol.*, 2023, **194**, 105484.
- 45 Y. Ren, D. Li, S. Jiang, *et al.*, Integration of transcriptomic and proteomic data reveals the possible action mechanism of the antimicrobial zhongshengmycin against *Didymella segeticola*, the causal agent of tea leaf spot, *Phytopathology*, 2021, **111**(12), 2238–2249.
- 46 M. Li, Z. Chen, X. Zhang, *et al.*, Enhancement of avermectin and ivermectin production by overexpression of the maltose ATP-binding cassette transporter in *Streptomyces avermitilis*, *Bioresour. Technol.*, 2010, **101**, 9228–9235.
- 47 T. Adékambi, T. M. Shinnick, D. Raoult, *et al.*, Complete *rpoB* gene sequencing as a suitable supplement to DNA-DNA hybridization for bacterial species and genus delineation, *Int. J. Syst. Evol. Microbiol.*, 2008, **58**, 1807–1814.
- 48 Q. L. Zhao, Y. Wang, J. H. Du, *et al.*, One new polyketone from the rice fermentation of *Xylaria longipes*, *Nat. Prod. Res.*, 2025, **37**(01), 52–56.
- 49 L. M. Naughton, S. Romano, F. O'Gara, *et al.*, Identification of secondary metabolite gene clusters in the *Pseudovibrio* genus reveals encouraging biosynthetic potential toward the production of novel bioactive compounds, *Front. Microbiol.*, 2017, **8**, 1494.
- 50 J. S. Yi, J. M. Kim, M. K. Kang, *et al.*, Whole-genome sequencing and analysis of *Streptomyces* strains producing multiple antinematode drugs, *BMC Genom.*, 2022, **23**(1), 610.
- 51 J. Y. Cha, S. Han, H. J. Hong, *et al.*, Microbial and biochemical basis of a *Fusarium* wilt-suppressive soil, *ISME J.*, 2016, **10**(1), 119–129.
- 52 G. Gao, F. Liu, Z. Xu, *et al.*, Evidence of nigericin as a potential therapeutic candidate for cancers: A review, *Biomed. Pharmacother.*, 2021, **137**, 111262.
- 53 X. Zhu, A. Hong, X. Sun, *et al.*, Nigericin is effective against multidrug resistant gram-positive bacteria, persisters, and biofilms, *Front. Cell. Infect. Microbiol.*, 2022, **12**, 1055929.
- 54 N. Lee, S. Hwang, W. Kim, *et al.*, Systems and synthetic biology to elucidate secondary metabolite biosynthetic gene clusters encoded in *Streptomyces* genomes, *Nat. Prod. Rep.*, 2021, **38**(7), 1330–1361.

